Available online at www.sciencedirect.com
SCIENCE DIRECT®
Nuclear Instruments and Methods in Physics Research A 497 (2003) 331–339
NUCLEAR INSTRUMENTS & METHODS IN PHYSICS RESEARCH Section A
www.elsevier.com/locate/nima

A systematic study of large PMTs for the Pierre Auger Observatory

A.K. Tripathi*, S. Akhanjee, K. Arisaka, D. Barnhill, C. D'Pasquale, C. Jillings, T. Ohnuki, P. Ranin

Department of Physics and Astronomy, University of California, 405 Hilgard Avenue, Los Angeles, CA 90095, USA

Received 17 June 2002; received in revised form 16 September 2002; accepted 7 October 2002

Abstract

In order to select the most suitable Photomultiplier Tubes (PMTs) for the surface detectors of the Pierre Auger Observatory, we have performed extensive tests on large PMTs from three different manufacturers: Electron Tubes Limited, Hamamatsu Photonics, and Photonis Imaging Sensors. We have developed specialized instrumentation to accurately measure the PMT characteristics such as gain, dark current, single photoelectron spectrum, dark pulse rate, afterpulse ratio, quantum efficiency, and linearity. The instrumentation and techniques used for these measurements and their results are reported.

PACS: 29.40.Ka; 29.40.Vj

Keywords: PMTs; Photodetectors; Water Cherenkov; Cosmic rays; Astroparticle physics

1. Introduction

The Pierre Auger Observatory is a large-area hybrid detector designed to collect a high-statistics sample of ultra-high-energy cosmic rays (UHECR), with energies greater than 10^{19} eV. The Pierre Auger Observatory consists of two detectors, one each in the northern and the southern hemispheres, respectively. The detector is described in detail elsewhere [1–8]. Briefly, each observatory consists of 1657 surface detectors (SD), and four flourescence detectors (FD). Each SD is a cylindrical water tank of 3.6 m diameter, and is 1.2 m deep. The interior of these tanks is lined with white diffuse tyvek sheet. The cosmic rays, after intereacting with the atmosphere, give rise to extended air showers in the air. The charged shower particles reaching the ground produce Cherenkov light in the water. This Cherenkov light is then detected by three Photomultiplier Tubes (PMTs), mounted symmetrically on top of each tank, with the photocathode looking vertically downward. The SDs are arranged on a hexagonal grid, with a spacing of 1.5 km. This array of SDs is viewed by four fluorescence detectors located along the periphery of the array,

*Corresponding author.
E-mail address: arun@physics.ucla.edu (A.K. Tripathi).

0168-9002/03/$ - see front matter
PII: S0168-9002(02)01792-8

providing an independent measurement of primary energy as well as the longitudinal shower profile for a subset of the data. Currently, the southern observatory is under construction near the town of Malargue in Mendoza province of Argentina [9].

2. Relevant PMT properties for Auger surface detectors

As mentioned above, the PMTs used in Auger SDs are required to detect the Cherenkov light produced by charged particles in water. After transmission through water and reflection from tyvek, the Cherenkov spectrum peaks in the 350–450 nm range in an SD. As a result, the SD PMTs must have good Quantum Efficiency (QE) in this wavelength range.

Low dark pulse rate and dark current are required in order to ensure the survival of the PMTs over the 20 year lifespan of the Auger experiment. In addition, since the arrival times of the shower particles at the ground can be spread over several microseconds, the PMT afterpulses can hide underneath the signal giving an erroneous measurement of the shower energy. As a result, low levels of afterpulsing are required.

The intrinsic spread in the arrival times of the particles at a given SD is greater than 100 ns, and also, individual SDs are separated by 1.5 km. As a result, fast timing is not required in Auger SD PMTs.

The PMT signals are digitized with 40 MHz Flash ADCs (FADC), with 15 bits of effective dynamic range. The operating gain of these PMTs must be low enough such that the ADCs do not saturate for the large signals expected from very high energy showers. At the same time, the gain must be high enough such that the signal resulting from a single muon is well above the electronic noise level, since the muons are used to calibrate the SDs. MC studies of the expected range of signals in Auger SDs and the measured level of electronic noise show that the optimum operating gain of these PMTs is $\sim 2 \times 10^5$.

Good linearity is the most important PMT requirement for the Auger SDs, because the highest energy showers resulting in large PMT signals are also of the greatest physics interest. Monte Carlo simulations indicate that the highest energy showers in Auger can give rise to peak signals as large as 50,000 photoelectrons per 25 ns approximately 500 m from the shower core. The SD PMTs, therefore, must be linear up to such large signals.

The 8 and 9 in. PMTs already available in the market were designed mainly for neutrino experiments, such as AMANDA, ICECUBE, and SNO, etc. As a result, they were optimized for high-gain ($> 10^7$) operation, in order to detect small signals, ranging from single photoelectron (SPE) to a few photoelectrons. In order to achieve the dynamic range needed in Auger, these PMTs must be operated at gains much below their optimal values,

Table 1
Dynode information for the three candidate PMTs optimized for Auger project

Manufacturer	PMT model	PMT bulb diameter	Dynode information
ETL	D731KB	200 mm	10 dynode stages Linear focus
Hamamatsu	R5912MOD	200 mm	8 dynode stages Linear focus
Photonis	XP1805/D1	230 mm	8 dynode stages Linear focus, Foil first dynode

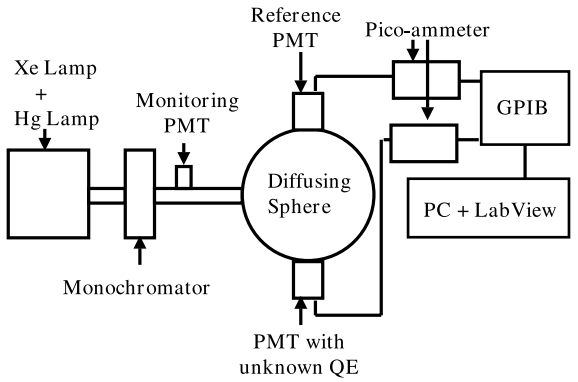

Fig. 1. A schematic of the quantum efficiency setup.

thus compromizing their linearity. This loss in linearity directly affects the energy measurement of the highest energy showers.

Mainly based on the above considerations for linearity over a large dynamic range at low gain, the Auger project requested three different vendors (Electron Tubes Limited (ETL), Hamamatsu, and Photonis) to manufacture sample candidate PMTs designed to satisfy the specifications for the Auger SDs, as described in the next section.

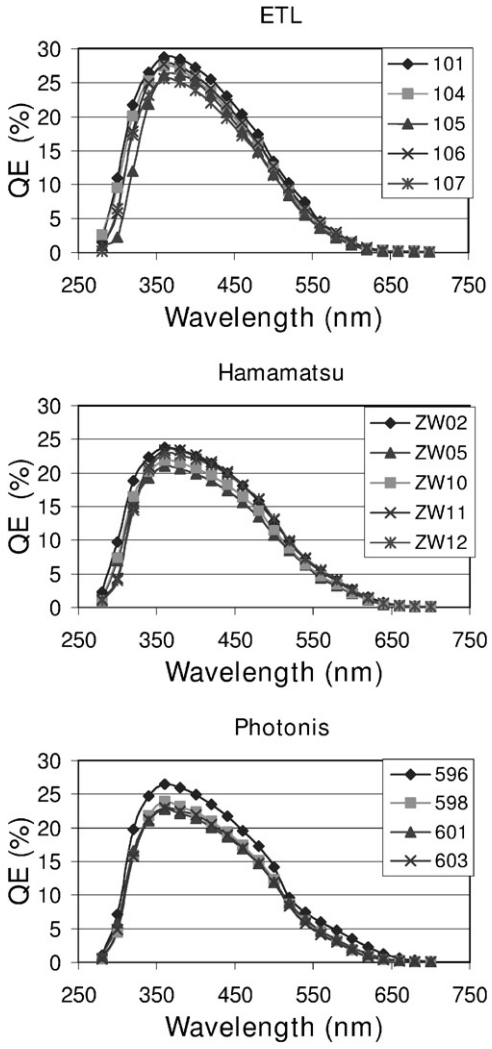

Fig. 2. Quantum efficiency as a function of wavelength for ETL 731KB, Hamamatsu R5912MOD, and Photonis XP1805/D1 PMTs. The solid lines are only to guide the eye.

3. Auger SD PMT specifications

Based on the considerations mentioned above, the following specification were provided to the three companies for manufacturing the new sample PMTs for Auger SDs:

- Cathode sensitivity:
  - Sk > 50 μA/lm.
  - Skb > 7 μA/lm-B (equivalent to QE > 16% at 420 nm).
  - QE at 350 nm > 16%.
- Gain and supply high voltage:
  - Standard operating gain $= 2 \times 10^5$.
  - High voltage must be less than 2000 V for the gain of 10^6.
- Dark current
  - $I_{\mathrm{Dark}}(\mathrm{Gain} = 1 \times 10^6) < 20$ nA.
  - $I_{\mathrm{Dark}}(\mathrm{Gain} = 1 \times 10^6)/I_{\mathrm{Dark}}(\mathrm{Gain} = 2 \times 10^5) < 10$.
- Dark pulse rate and afterpulse ratio:
  - Dark pulse rate, measured with 0.25 PE threshold after 2 h in dark at a gain of 10^6 must be less than 10 kHz.
  - Afterpulse ratio, defined as the charge in a time window 200–5000 ns after the

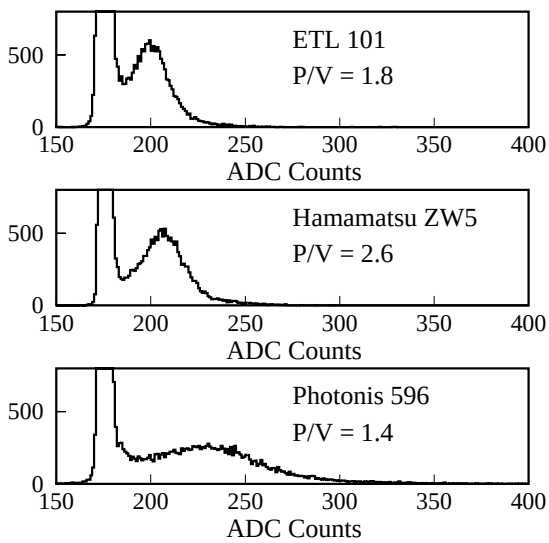

Fig. 3. Sample single photoelectron spectra for ETL 731KB, Hamamatsu R5912MOD, and Photonis XP1805/D1 PMTs. The spectra shown here are the ones with the largest peak-to-valley ratio for each kind of PMT.

main pulse, measured as the fraction of the charge in the main pulse at a gain of 10^6, must be less than 5%.

- Pulse linearity:
  - At a gain of 2×10^5, the PMT must be linear within $\pm 5\%$ up to 50 mA of anode current.
- SPE resolution (measured at Gain $\geqslant 10^6$):
  - Peak to valley ratio > 1.2.
- Time resolution for single PE (measured at Gain $\geqslant 10^6$):
  - Transit Time Spread (FWHM) <10 ns.
  - Rise time (10–90%) <6 ns.

4. The candidate PMTs

During the spring of 2001, ETL, Hamamatsu, and Photonis manufactured the new sample PMTs according to the Auger specifications. The PMT model numbers and the dynode structure information for the PMTs tested are listed in Table 1.

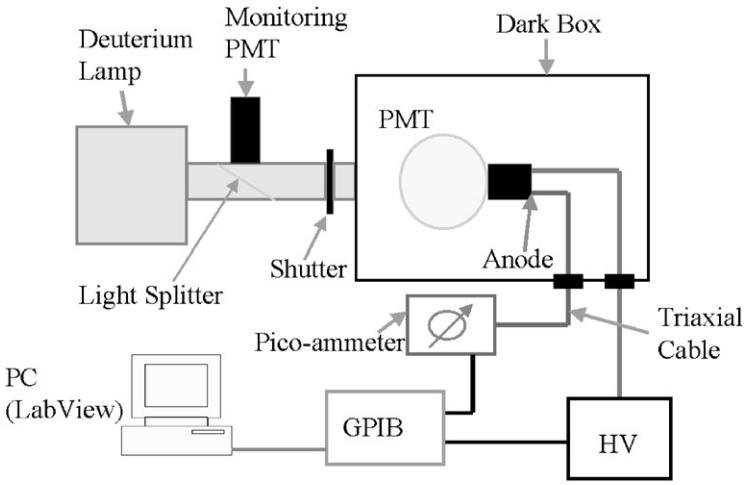

Fig. 4. Schematic of the setup used for gain and dark current measurements.

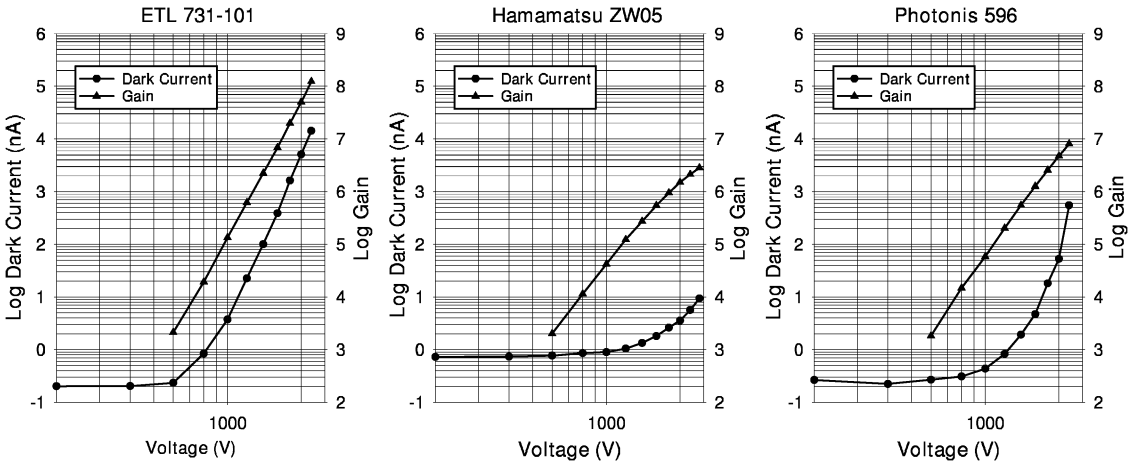

Fig. 5. Sample gain and dark current curves for ETL 731KB, Hamammatsu R5912MOD, and Photonis XP1805/D1 PMTs. Solid lines are only to guide the eye.

5. Measurements

After procuring the PMTs from the manufacturers, we performed an extensive battery of tests on them. The measurement techniques and their results are described below.

5.1. Quantum efficiency

Fig. 1 shows a schematic of the experimental setup used to measure the QE of the PMTs. The light source was an Oriel model 6291 Xe arc lamp set inside an Oriel model 7340 housing. The lamp was powered by an Oriel model 68806 power supply. The light first passed through a computer controlled monochromator (Oriel 77250), which was used to select a particular wavelength. The monochromator was calibrated using a mercury lamp, also situated in the same housing that holds the Xe lamp. After the monochromator, light passed through a variable slit, and then through a 50/50 splitter. Part of the light from the splitter went to an Oriel model 7060 PMT assembly for monitoring the stability of the light source. The remaining part of the light went into the so-called integrating sphere. It is a sphere with diffuse white interior walls with two diametrically opposite 1.25 in. diameter openings. The integrating sphere diffuses the incident light such that the intensity of photons incident over the two openings is the same within 1%.

This setup is designed to measure the QE by comparing the photocathode current of a PMT with unknown QE to that of a reference PMT, whose QE is known independently, e.g., from a PMT manufacturer. We used a Hamamatsu R6234 hexagonal PMT as reference. The QE curve of this PMT was already known from Hamamatsu measurements. For a fixed light intensity and wavelength, if the measured photocathode currents from the reference and subject PMTs are I_{ref} and I_s, respectively, then the QE of the subject PMT is given by

$$QE_s = QE_{ref} \times (I_s/I_{ref}) \quad (1)$$

where QE_{ref} is the known QE of the reference PMT. The results of the QE measurements are shown in Fig. 2. All three different kinds of PMTs satisfy the Auger QE specifications in the 350–450 nm wavelength region. ETL PMTs show the highest peak QE.

5.2. Single photoelectron spectrum

The measurement of SPE spectrum is required in order to determine the absolute gain of the

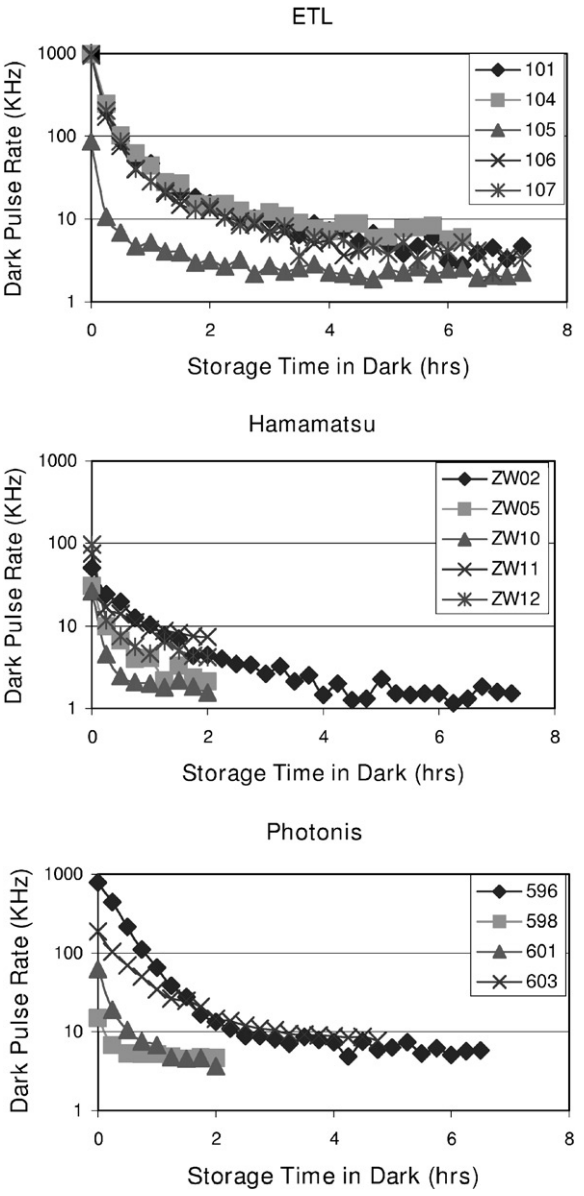

Fig. 6. Dark pulse rate as a function of storage time in dark for ETL 731KB, Hamamatsu R5912MOD and Photonis XP1802/D1 PMTs. Solid lines are only to guide the eye.

PMT. The light source used for this purpose was a Hamamatsu pico second laser (PLP-01), which also provided an NIM signal synchronous with the laser pulses. Before reaching the PMT, the light passed through a neutral density filter wheel, and then through a diffuser. The filter wheel could provide continuous light attenuation by up to a factor of 10,000. The PMT was operated at a gain of approximately 10^6, and the anode signal was amplified by a factor of 42, before being digitized by a LeCroy 2249W ADC. The NIM signal from the laser was used to gate the ADC. The data acquisition system was written in LabView, running on a PC with Windows 98 operating system. The amount of light reaching the PMT was reduced until approximately 90% of the laser pulses resulted in pedestal, and only 10% of the pulses gave rise to signal above the pedestal. This ensures that any signal observed above the pedestal is predominantly from SPEs. If the average number of photoelectrons emitted from the photocathode in each laser pulse is μ, then, the probability of observing exactly 0 photoelectrons in a given pulse is $P(0) = e^{-\mu}$. Since only 10% of the laser pulses result in any signal, $P(0) = 0.9 = e^{-\mu}$, and hence $\mu = 0.1$. It follows that in any signal observed above pedestal, $P(\text{npe} = 1)/P(\text{npe} > 1) \simeq 20$, where npe is the number of photoelectrons. Fig. 3 shows SPE spectra with the best peak-to-valley ratio for each kind of PMTs. Fig. 9 lists the peak-to-valley ratios from all measurements. Clearly, all the PMTs satisfy Auger SPE specifications.

5.3. Gain and dark current

The PMT gain and dark current as a function of the applied high voltage were measured using the setup shown in Fig. 4. The light source was a highly stable Hamamatsu L1403 deuterium lamp. The light from the lamp passed through a slit, followed by a 50–50 splitter, and then through a remote controlled shutter before entering the dark box. The PMT anode current was measured by a Keithly 486 picoammeter. The high voltage to the PMT was supplied by a Stanford Research Systems model PS325 power supply. Both the high-voltage power supply and the picoammeter were read out using a GPIB interface and LabView-based software.

In order to measure the dark current, the shutter to the dark box was closed, and the PMT was allowed to cool down for 30 min at −1500 V inside the dark box. Then the high voltage on the PMT was changed from −800 to −2200 V in 200 V steps, and the anode current was measured at each voltage.

In order to measure the gain as a function of the applied high voltage, the shutter was opened and the intensity of light was adjusted such that the anode current at −2200 V was less than 1% of the current drawn by the PMT base, thus ensuring linear behavior even at the highest applied voltage. Then the anode current was measured as a function of the applied high voltage. This yields only a relative gain measurement, since the photocathode current was not measured.

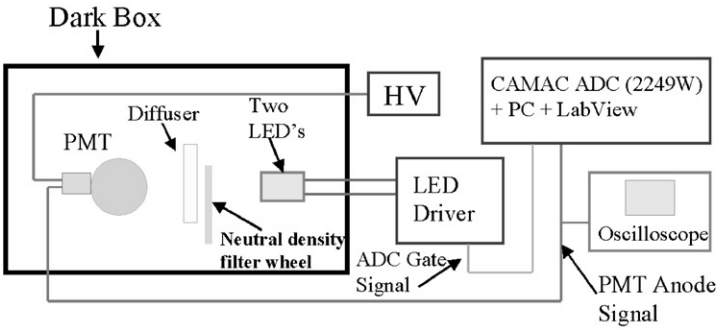

Fig. 7. A schematic of the linearity setup.

However, the absolute gain for each PMT was measured at a known voltage from the SPE spectrum, and this one point can be used to convert this relative gain measurement into an absolute one.

Typical gain and dark current curves for the three kinds of PMTs are shown in Fig. 5. The HVs required for gains of 2×10^5 and 10^6 as well as measured dark currents at a gain of 10^6 after 30 min in dark for all the PMTs are listed in Fig. 9. Hamamatsu shows the lowest dark currents for a given gain.

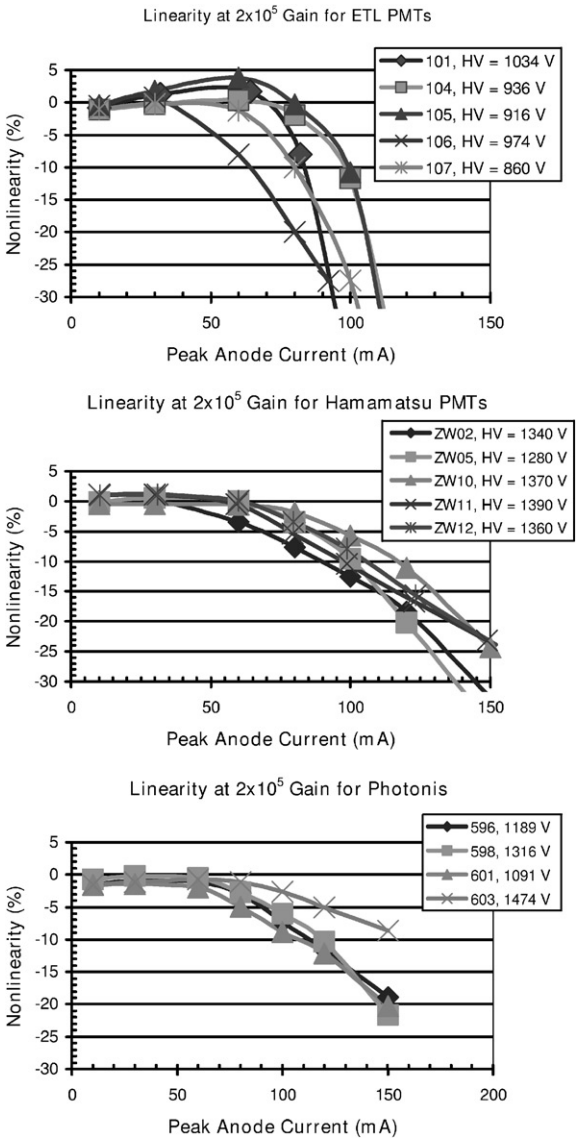

Fig. 8. Linearity as a function of peak anode current for ETL 731KB, Hamamatsu R5912MOD, and Photonis XP1805/D1 PMTs. Solid lines are only to guide the eye.

5.4. Dark pulse rate

Even in the absence of any light incident on the PMT, electrons are emitted from the photocathode because of thermionic emission and residual radioactivity in the glass, etc., giving rise to single PE pulses at the anode. These are known as dark pulses. A low dark pulse rate is desirable to reduce extraneous contributions to the signals of interest as well as for the longevity of the PMT.

In order to measure the dark pulse rate, the PMT was briefly exposed to the ambient light in the lab and then placed in the dark box. The high voltage for a gain of 10^6 was then applied to the PMT. The anode signal was amplified by a factor of 42, and the resulting dark pulses were digitized using a LeCroy 2249W ADC. Offline, only the pulses above 0.25 PE threshold were counted. The dark pulse rates were measured as a function of time for each PMT, and the results are shown in Fig. 6. Measured dark pulse rates after 2 h in dark for each PMT are also listed in Fig. 9. Hamamatsu shows the lowest dark pulse rate while ETL PMTs show the noisiest behavior.

5.5. Afterpulse ratio

The residual gases inside a PMT can be ionized by the accelerating electrons produced from a light pulse, and these ions, being positively charged, travel to the photocathode and cause a secondary pulse, known as an afterpulse. The delay between the main pulse and the afterpulses depends on the mass of the ion, the applied high voltage, and the size of the PMT. A measure of afterpulsing in a PMT is the afterpulse ratio (APR), defined as

$$\mathrm{APR} = \frac{Q_{\mathrm{Afterpulse}}}{Q_{\mathrm{main}}} \tag{2}$$

where Q_{main} is the total charge contained in the anode pulse resulting from incident light pulse on the PMT, and $Q_{\mathrm{Afterpulse}}$ is the total charge contained in the afterpulses. In our case, the main

pulse had a FWHM of 80 ns, and the afterpulses were defined as any pulses between 200 and 5000 ns from the leading edge of the main pulse.

Since the signals resulting from extensive air showers are spread over several microseconds, an afterpulse can easily hide in the signal, and result in an erroneous measurement of the energy. Therefore, low level of APR is desirable.

In our afterpulsing measurements, the PMTs were operated at a gain of 10^6, and a blue (450 nm) LED was used as a light source. The measured afterpulse ratios are listed in Fig. 9. All the PMTs satisfy Auger specifications on afterpulsing. Photonis shows the lowest level of afterpulsing.

5.6. Linearity

A schematic of the experimental setup used to measure the linearity is shown in Fig. 7. The LED pulser used for linearity measurements consisted of two LEDs (say A and B), which were pulsed in the following sequence: A alone, B alone, and then (A + B) simultaneously. The pulser also provided a synchronous gate signal, which, after appropriate delays, was used to gate the LeCroy 2249W ADC.

Let X be the PMT signal (total charge in the PMT anode pulse) corresponding to the case when only LED A fires; Y the PMT signal corresponding to the case when only LED B fires; and Z the PMT signal when both LED A and LED B fire simultaneously. Then, if the PMT is linear, $Z = X + Y$. We define the non-linearity of the PMT as

$$\mathrm{NL} = \frac{Z - (X + Y)}{(X + Y)}. \tag{3}$$

The results of linearity measurements at 2×10^5 gain are shown in Fig. 8, and are also listed in Fig. 9. ETL shows some overlinearity, and then a rapid loss in linearity at anode currents in excess of 50 mA. Photonis shows the most linear behavior. All three kinds of PMTs, however, satisfy the Auger requirements on linearity.

6. Summary

We have performed extensive tests on large PMTs from ETL, Hamamatsu and Photonis in order to determine their suitability for the SDs of the Pierre Auger Observatory. We have developed dedicated instrumentation to measure PMT characteristics such as QE, gain, dark current, SPE spectra, afterpulse ratio, dark pulse rate, and linearity. Results of these tests are summarized in Fig. 9. Photonis XP1805 was finally selected by the Auger collaboration for use in the SDs.

PMT Type and Serial Number	HV (V) for 2×10^5 (10^6) Gain	I_D (nA) at 10^6 Gain	$I_D(10^6)$ / $I_D(2\times10^5)$	P/V Ratio	Non-linearity (%) for 50 mA at 2E5 Gain	Peak Anode Current (mA) for -5% Non-linearity at 2E5 gain	Dark Pulse Rate (KHz) (0.25 PE Thr.)	Afterpulse Ratio (%)	QE (%) at 350 nm	QE (%) at 420 nm
Hamamatsu										
ZW02	1340 (1940)	5.0	3.3	1.9	-2.5	65	4.5	1.2	23.1	21.4
ZW05	1280 (1830)	3.0	2.5	2.6	0.0	85	2.1	1.4	20.1	18.8
ZW10	1370(2000)	4.0	2.6	1.3	-0.5	95	1.6	2.6	21.0	19.7
ZW11	1390(2000)	1.3	3.2	1.5	0.5	80	7.3	3.4	22.2	21.6
ZW12	1360(1940)	0.9	2.6	1.7	0.7	90	4.2	2.8	21.6	21.2
ETL										
101	1034(1276)	36.5	6.5	1.8	1.7	80	10.9	3.9	27.6	25.4
104	936(1164)	18.6	3.8	1.4	0.0	90	23.7	2.1	26.4	23.7
105	916(1098)	6.0	2.6	1.4	3.8	80	3.1	3.0	24.0	23.1
106	974(1127)	17.5	4.2	1.4	-4.5	50	15.2	4.0	26.3	24.2
107	860(1025)	5.2	3.2	1.8	0.0	70	11.8	2.8	24.4	22.0
Photonis										
596	1200(1540)	3.0	3.8	1.4	-1.2	85	15.2	0.6	25.5	23.5
598	1316(1700)	5.7	2.7	1.2	-1.2	90	4.7	1.3	22.8	21.0
601	1090(1405)	2.4	2.4	1.2	-2.0	75	3.7	3.5	21.8	20.1
603	1490(1993)	11.0	3.6	1.3	-1.2	105	17.1	2.1	22.1	20.5

Fig. 9. Summary of all the PMT measurements.

References

[1] M.T. Dova, Survey of the Pierre Auger observatory, Proceedings of the 27th International Cosmic Ray Conference, 7–15 August 2001, Hamburg, Germany.
[2] J. Lloyd-Evans, Aperture and precision of the Auger surface detector, Proceedings of the 27th International Cosmic Ray Conference, 7–15 August 2001, Hamburg, Germany.
[3] R. Cester, The Aperture, sensitivity, and precision of the Auger flourescence detector, Proceedings of the 27th International Cosmic Ray Conference, 7–15 August 2001, Hamburg, Germany.
[4] B. Dawson, The Hybrid aperture and precision of the Auger observatory, Proceedings of the 27th International Cosmic Ray Conference, 7–15 August 2001, Hamburg, Germany.
[5] H. Gemmeke, The Auger fluorescence detector electronics, Proceedings of the 27th International Cosmic Ray Conference, 7–15 August 2001, Hamburg, Germany.
[6] J.A. Matthews, Atmospheric monitoring for the Auger fluorescence detector, Proceedings of the 27th International Cosmic Ray Conference, 7–15 August 2001, Hamburg, Germany.
[7] T. Suomijarvi, Surface detector electronics for the Auger observatory, Proceedings of the 27th International Cosmic Ray Conference, 7–15 August 2001, Hamburg, Germany.
[8] P.D.J. Clark, D. Nitz, Communications in the Auger observatory, Proceedings of the 27th International Cosmic Ray Conference, 7–15 August 2001, Hamburg, Germany.
[9] I. Allekotte, A. Barbosa, J. Kleinfeller, Status of the engineering array, Proceedings of the 27th International Cosmic Ray Conference, 7–15 August 2001, Hamburg, Germany.